

# Influence of Substrate Temperature and Nitrogen Gas on Zinc Nitride Thin Films Prepared by RF Reactive Sputtering\*

Zhang Jun<sup>1,2</sup>, Xie Erqing<sup>1</sup>, Fu Yujun<sup>1</sup>, Li Hui<sup>1</sup>, and Shao Lexi<sup>2,†</sup>

(1 School of Physical Science and Technology, Lanzhou University, Lanzhou 730000, China)

(2 School of Physics, Zhanjiang Normal College, Zhanjiang 524048, China)

**Abstract:** Zinc nitride ( $Zn_3N_2$ ) thin films were prepared by radio frequency (RF) magnetron sputtering on quartz glass at different substrate temperatures. The structure and composition were characterized by X-ray diffraction and Raman-scattering measurements, respectively. The polycrystalline phase  $Zn_3N_2$  films appeared when the ratio of the  $N_2$  partial pressure to the total pressure reached 1/2. The effects of the substrate temperature on the electrical and optical properties of the  $Zn_3N_2$  films were investigated by Hall measurements and optical transmission spectra. The electrical and optical properties of the films were highly dependent on the substrate temperature. With the substrate temperature increasing from 100 to 300°C, the resistivity of the  $Zn_3N_2$  films decreased from 0.49 to 0.023  $\Omega \cdot cm$ , the carrier concentration increased from  $2.7 \times 10^{16}$  to  $8.2 \times 10^{19} cm^{-3}$ , and the electron mobility decreased from 115 to 32  $cm^2/(V \cdot s)$ . The deposited  $Zn_3N_2$  films were considered to be n-type semiconductors with a direct optical band gap, which was around 1.23 eV when the substrate temperature was 200°C.

**Key words:** zinc nitride; thin film; magnetron sputtering; electrical and optical properties

**EEACC:** 0520B

**CLC number:** O484.1

**Document code:** A

**Article ID:** 0253-4177(2007)08-1173-06

## 1 Introduction

Zinc compounds have been the subject of intensive research and development efforts during the last few decades because of their wide direct band gaps and potential applications in visible and UV optoelectronic technologies. Among them, zinc oxide (ZnO) has important application potential owing to its unique properties. Its wide band gap of 3.37 eV and exciton binding energy of 60 meV at room temperature make ZnO suitable for short wavelength opto-electronic devices, including light-emitting diodes (LEDs), laser diodes (LDs), and room-temperature UV laser devices<sup>[1,2]</sup>. Zinc phosphide ( $Zn_3P_2$ ), with a direct gap of near 1.51 eV, is a promising material for low cost solar cells<sup>[3]</sup>. Zinc sulphide (ZnS) is considered to be the key material for applications in light-emitting diodes (LEDs) and laser diodes (LDs) in the ultraviolet (UV) range of the spec-

trum because of its band gap of 3.73 eV at room temperature<sup>[4~6]</sup>. Semiconductor nitrides such as aluminum nitride (AlN) and gallium nitride (GaN) can be considered as promising materials for their potential in optical devices or high speed and high-power electronic devices due to their characteristics of wide band gap, high electron saturation velocity, and high breakdown voltage<sup>[7,8]</sup>. As with the materials above,  $Zn_3N_2$  is also a direct band gap and n-type semiconductor with cubic antixbyite structure. Therefore,  $Zn_3N_2$  also has important application potential due to its significant electrical and optical properties<sup>[9~13]</sup>. In addition, many groups have already succeeded in forming p-type ZnO films by thermal oxidation of  $Zn_3N_2$  films<sup>[14,15]</sup>. However, different values of its physical properties and different preparation techniques of  $Zn_3N_2$  have been reported. For instance, the band gap energy was reported to be 3.2 eV by Kuriyama<sup>[10]</sup>, 1.23 eV by Futsuhara<sup>[11]</sup> and 1.01 eV by Toyoura<sup>[12]</sup>. Among many prepara-

\* Project supported by the Natural Science Foundation of Guangdong Province (No. 31927) and the Research Foundation of Education Bureau of Guangdong Province (No. 粤财教[2006]112)

† Corresponding author. Email: shaolxmail@163.com

Received 7 February 2007, revised manuscript received 24 March 2007

©2007 Chinese Institute of Electronics

tion techniques, reactive RF magnetron sputtering has been used to grow high quality stoichiometric nitrides because the plasma can provide sufficient active nitrogen species at low substrate temperature.

In this work, RF planar magnetron sputtering was employed to prepare polycrystalline  $Zn_3N_2$  thin films on quartz glass. The crystal structure of the films investigated by X-ray diffraction (XRD) was dependent on the  $N_2$  concentration in sputtering ambient and the substrate temperature. In addition, the effects of the substrate temperature on the electrical and optical properties of the  $Zn_3N_2$  films were investigated.

## 2 Experiment

$Zn_3N_2$  films were prepared on quartz glass substrates by reactive magnetron sputtering with a conventional RF (13.56MHz) sputter setup. The background pressure of the sputtering chamber was evacuated below  $1 \times 10^{-4}$  Pa with a turbo molecular pump. The quartz glass substrates were ultrasonically cleaned in acetone, rinsed in alcohol, and then dried in hot air. A metallic zinc disc (purity of 99.999%) of 60mm in diameter was used as the target. The target-substrate distance was maintained at 60mm. The sputtering time was 30min and the RF power was kept at 50W. Before film deposition, the target was sputter-etched in Ar plasma for 30min to remove contamination.  $N_2$ -Ar mixtures were used as sputtering ambient. The  $N_2$  and Ar gases were introduced into the sputtering chamber through the individual mass flow controllers. The total flow rate and total pressure were 40sccm and 1.2Pa, respectively. Meanwhile, the nitrogen partial pressure varied from 0.12 to 0.96Pa. The substrates can be heated up to 300°C, as measured by a thermocouple fixed beside the samples. In order to study the effects of the ratio of the  $N_2$  partial pressure to the total pressure ( $P_N/P_T$ ) and the substrate temperature, two series of experiments were performed. First, the substrate temperature was fixed at 200°C, while the ratio of the  $N_2$  partial pressure to the total pressure ( $P_N/P_T$ ) was varied from 1/10 to 4/5. Secondly, the  $P_N/P_T$  was fixed at 1/2, while the substrate temperature was varied and other growth parameters were held constant.

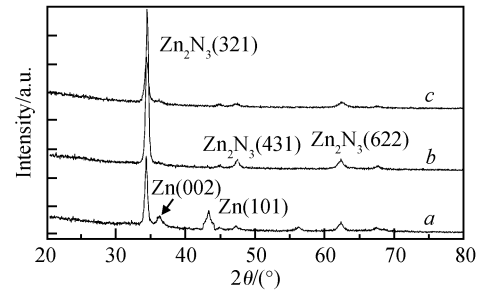


Fig. 1 X-ray diffraction patterns of the thin films deposited at the various ratios of the  $N_2$  partial pressure to the total pressure  $P_N/P_T$  of 1/5 (a), 1/2 (b), and 4/5 (c). Substrate temperature was 200°C.

The crystallographic properties of the thin films were investigated by an X-ray diffraction system (Rigaku D/Max-IIIC, with a wavelength of 0.1542nm). The surface morphologies and thickness of the gold coated thin films were characterized by scanning electron microscopy (SEM Hitachi S-4800). Raman-scattering measurements (HORIBA Jobin Yvon HR800) were conducted in the wave number range of  $100 \sim 1200\text{cm}^{-1}$ . The 488nm line of an  $Ar^+$  ion laser was used for excitation, and the incident laser power was 1mW. The electrical properties of the film were examined by Hall measurements using the van der Pauw configuration and hot-probe measurements. The ohmic contacts were fabricated by evaporating aluminum at the four symmetrical corners of the samples, which were then annealed at 350°C in Ar flow for 2h. Optical transmission spectra were measured by a double beam spectrometer (Hitachi U-3500). A clean quartz glass was used for a reference sample. Absorption coefficient was calculated from the transmission spectrum with film thickness. All the above measurements were performed at room temperature.

## 3 Results and discussion

The crystal structure and orientation of the deposited thin films were investigated by XRD. Figure 1 shows the XRD patterns of the thin films prepared at different  $N_2$  concentrations. It can be seen from Fig. 1 that, besides the diffraction peak of the  $Zn_3N_2$  (321) ( $2\theta = 34.3^\circ$ ), there are also some other peaks at  $2\theta = 36.2^\circ$  and  $43.2^\circ$  arising from the metallic zinc with hexagonal close-packed crystal structure. This indicates that both

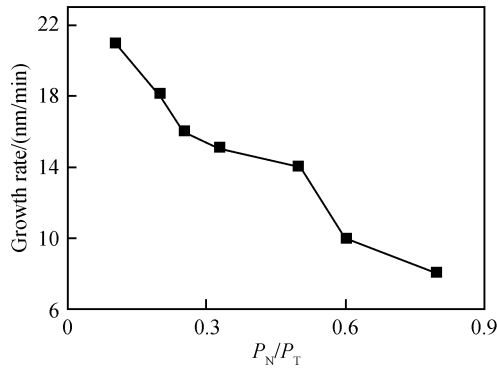


Fig.2 Film growth rate versus the ratio of the  $N_2$  partial pressure to the total pressure  $P_N/P_T$

$Zn_3N_2$  and Zn co-exist when  $P_N/P_T = 1/5$ . When  $P_N/P_T = 1/2$ , the peaks were attributed to the metallic Zn disappearance, indicating that the thin films prepared in this  $N_2$  concentration were in a polycrystalline phase. When the  $P_N/P_T$  is increased to  $4/5$ , the intensity of the dominating  $Zn_3N_2$  (321) peak decreases, and the other peaks arising from the  $Zn_3N_2$  (431) and (622) nearly disappear. But it should be pointed out that the (321) peak is still dominant, revealing a preferred orientation of the thin film. The results of the XRD analysis are different from the report of Futsuhara in Ref. [11], in which the dominating peak of  $2\theta = 36.7^\circ$  was attributed to  $Zn_3N_2$  (400). We think that the differences in the deposited parameters may be the main reasons for this disagreement, such as the substrate temperature, the sputtering power, and the substrate species. The results of the XRD analysis show that the  $P_N/P_T$  ratio affects the thin film texture greatly. When  $P_N/P_T$  is less than  $1/5$ , more sputtered zinc atoms reach the substrate than excited nitrogen species, so there are not enough excited nitrogen species reacting with the sputtered Zn atoms. Therefore, the deposited film showed two phases of  $Zn_3N_2$  and Zn. Increasing  $P_N/P_T$  from  $1/5$  to  $4/5$ , we get a single phase of  $Zn_3N_2$  with the preferred orientation. But the growth rate measured by cross section SEM micrograph decreases with increasing  $P_N/P_T$ , as shown in Fig. 2. This can be explained as follows. At a fixed sputtering gas pressure, a higher  $P_N$  means a lower  $P_{Ar}$ , resulting in a lower sputtering yield from the zinc target, because the sputtering rate of  $Ar^+$  is larger than that of  $N^{2+}$ .

In order to investigate the effects of the substrate temperature on the crystallizability and the

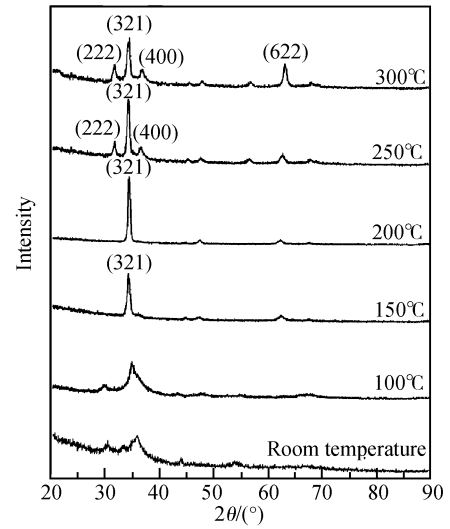


Fig.3 X-ray diffraction patterns of thin films deposited at various substrate temperatures  $P_N/P_T$  was  $1/2$ .

orientation of the thin films, the films were deposited at various substrate temperatures when  $P_N/P_T$  was fixed at  $1/2$ . Figure 3 shows the XRD patterns of the thin films prepared at various substrate temperatures. It can be seen that when the substrates were at room temperature or  $100^\circ C$ , the deposited thin films were amorphous  $Zn_3N_2$ . As the substrate temperature is increased from  $100$  to  $200^\circ C$ , the  $Zn_3N_2$  (321) peak at  $2\theta = 34.3^\circ$  becomes dominant, and the film shows  $Zn_3N_2$  (321) preferred orientation. When the substrate temperature is increased to  $300^\circ C$ , the  $Zn_3N_2$  (222), (400) and (622) peaks at  $2\theta = 31.7^\circ, 36.8^\circ$  and  $63.1^\circ$  appear in the patterns, indicating that the deposited  $Zn_3N_2$  thin films are polycrystalline films. The intensity and the full width at half-maximum (FWHM) of the  $Zn_3N_2$  (321) peak of the film deposited at  $200^\circ C$  are the highest and narrowest, respectively. We can evaluate the mean grain sizes (GS) of the thin films by Scherer's formula<sup>[15]</sup>:

$$GS = \frac{0.9\lambda}{B\cos\theta} \quad (1)$$

where  $\lambda$ ,  $\theta$ , and  $B$  are the X-ray wavelength ( $0.154\text{nm}$ ), the Bragg diffraction angle, and the full width at half-maximum of the (321) peak, respectively. The calculated grain sizes of the samples are  $76, 56$ , and  $44\text{nm}$  for the samples deposited at  $200, 250$ , and  $300^\circ C$ , respectively.

Figure 4 shows the Raman spectra of the thin films deposited at various substrate temperatures.

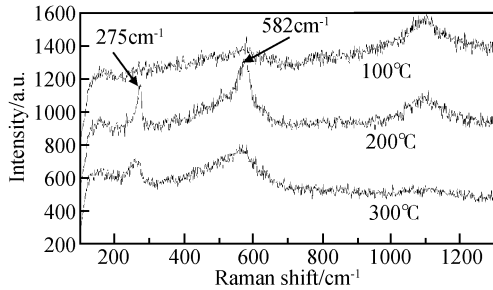


Fig.4 Raman spectra of the thin films deposited at various substrate temperatures  $P_N/P_T$  was 1/2.

In the measurement range of  $100\sim 1200\text{cm}^{-1}$ , the deposited thin films show two vibration peaks around  $275$  and  $582\text{cm}^{-1}$ . The predominant  $582\text{cm}^{-1}$  mode and the  $275\text{cm}^{-1}$  mode are local vibrational modes related with the vibrating nitrogen-related complexes<sup>[16,17]</sup>. As the substrate temperature is increased from  $100$  to  $300^\circ\text{C}$ , the intensity and shape of the peaks are changed noticeably. This indicates that the composition of the thin film is highly sensitive to the substrate temperature. The intensity of vibration peaks in the film deposited at  $200^\circ\text{C}$  is strongest. The kinematic energy of the sputtered species at  $200^\circ\text{C}$  substrate temperature may be sufficient to make nitrogen species react with the Zn atoms on the quartz glass substrates.

Figure 5 shows typical SEM images of the surface morphology of the samples prepared at various substrate temperatures. The surface morphology of the films changes significantly with increasing substrate temperature. The grains curve and form dendrite-like structures which intersect each other in the sample deposited at a substrate temperature of  $100^\circ\text{C}$ . The  $\text{Zn}_3\text{N}_2$  film was composed of uniform particles with  $70\text{nm}$  in size, as the substrate temperature increased to  $200^\circ\text{C}$ . When the sample was deposited at  $300^\circ\text{C}$ , the sizes of the grains became smaller than that of the sample deposited at  $200^\circ\text{C}$ , and the surface of the film became more compact and flat. The insert (d) of Fig. 5 shows an SEM cross sectional image of the sample deposited at  $200^\circ\text{C}$ ; there is no void between the film and the substrate. In addition, it was confirmed that the thickness of the film is about  $420\text{nm}$  compared with the interposed marker.

The hot-probe measurements indicate that all of the fabricated thin films exhibited n-type conductivity. Table 1 shows the results of the Hall measurements. As the substrate temperatures increased from  $100$  to  $300^\circ\text{C}$ , the resistivity ( $\rho$ ) of the  $\text{Zn}_3\text{N}_2$  film decreased from  $0.49$  to  $0.023\Omega\cdot\text{cm}$ , the carrier concentration ( $n_e$ ) increased from  $2.7\times 10^{16}$  to  $8.2\times 10^{19}\text{cm}^{-3}$ , and the electron mobility ( $\mu$ ) decreased from  $115$  to  $32\text{cm}^2/(\text{V}\cdot\text{s})$ . Therefore, the decrease in resistivity is attributed

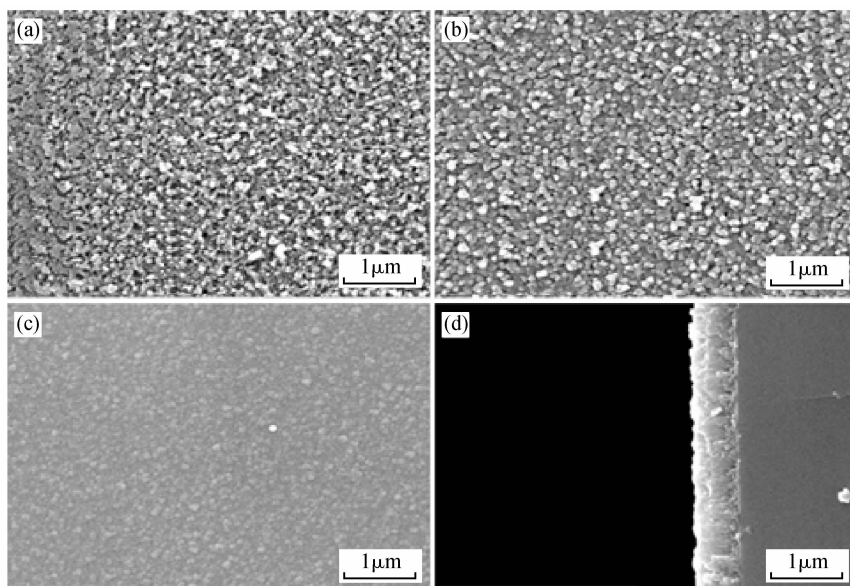


Fig.5 Typical SEM images of the samples prepared at various substrate temperatures (a)  $100^\circ\text{C}$ ; (b)  $200^\circ\text{C}$ ; (c)  $300^\circ\text{C}$ ; (d) Cross sectional image of (b)

Table 1 Results of the Hall effect measurements of the thin films deposited at various substrate temperatures  $P_N/P_T$  was 1/2.

Substrate temperature /°C	Resistivity /( $\Omega \cdot \text{cm}$ )	Mobility /( $\text{cm}^2/(\text{V} \cdot \text{s})$ )	Carrier concentration / $\text{cm}^{-3}$	Conductivity type
100	0.49	115	$-2.7438 \times 10^{16}$	n
150	0.12	96	$-4.127 \times 10^{17}$	n
200	0.056	83	$-6.4947 \times 10^{18}$	n
250	0.042	45	$-9.6537 \times 10^{18}$	n
300	0.023	32	$-8.2012 \times 10^{19}$	n

to the increase in the carrier concentration. The electron mobility decreased monotonically with increasing carrier concentration. The electron mobility is dominated both by ionized impurity scattering and by grain boundary scattering in polycrystalline semiconductor. In the deposited  $\text{Zn}_3\text{N}_2$  films, the electron mobility monotonically decreased with increasing carrier concentration. Furthermore, the results of the XRD analysis show that the sizes of the grains became smaller with increasing substrate temperature. It can be concluded that the electron mobility in the  $\text{Zn}_3\text{N}_2$  films is mainly dominated by the ionized impurity scattering, while the grain boundary scattering has little influence on the electron mobility.

The optical properties of the fabricated samples were evaluated by measuring the transmission spectra in the wavelength range of 550~1100nm using the spectrophotometer. Typical transmission spectra of the films deposited at various substrate temperatures are shown in Fig. 6. The fundamental absorption edge was located at around 1000nm. The transmittance rate of the films in the near infrared range is about 65%. The absorption

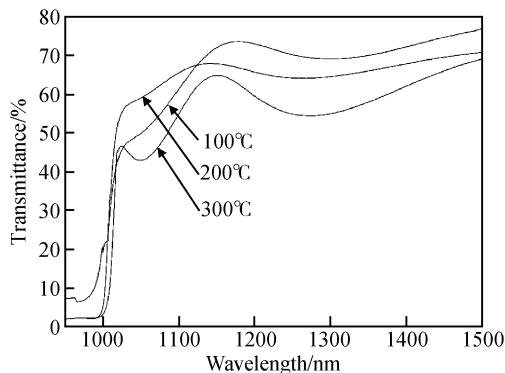


Fig. 6 Typical transmission spectra of films deposited at various substrate temperatures  $P_N/P_T$  was 1/2.

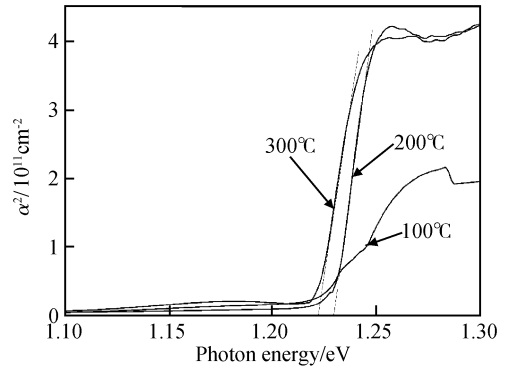


Fig. 7 Relation between squared absorption coefficient and photo energy of the films deposited at various substrate temperatures  $P_N/P_T$  was 1/2.

coefficient of the films can be calculated from the transmission spectrum with the film thickness. In order to check the band structure of the  $\text{Zn}_3\text{N}_2$  films, Figure 7 shows the absorption coefficient as a function of the photon energy. It can be seen that the relationship between the absorption coefficient and the photon energy of the films deposited at 200 and 300°C followed the equation

$$(\alpha h\nu)^2 = A(h\nu - E_g) \quad (2)$$

As for the absorption edge of semiconductors, Equation (2) is valid for the direct electron transition from valence to conduction bands. Therefore  $E_g$  was determined by extrapolating the linear part of these plots to  $\alpha = 0$ . The  $E_g$  of the films deposited at 200 and 300°C were calculated to be 1.23 and 1.22eV, respectively. In our work, the values of band gap energy agree well with the results reported by Futsuhara in Ref. [11] in spite of the differences in the deposited parameters such as the substrate temperature, the  $\text{N}_2$  concentration, or the substrate species.

## 4 Conclusions

Zinc nitride ( $\text{Zn}_3\text{N}_2$ ) thin films were prepared by radio frequency (RF) magnetron sputtering on quartz glass at various substrate temperatures. The polycrystalline single phase  $\text{Zn}_3\text{N}_2$  thin films were fabricated when the  $P_N/P_T$  exceeded 1/2. The structural, electrical and optical properties of the  $\text{Zn}_3\text{N}_2$  films were highly dependent on the substrate temperature. With the substrate temperature increasing from 100 to 300°C, the  $\text{Zn}_3\text{N}_2$  film changed from amorphous to highly ordered films, and the mean grain size of the samples de-

posited at 200°C was about 70nm. The resistivity of the Zn<sub>3</sub>N<sub>2</sub> film decreased from 0.49 to 0.023 Ω·cm, and the carrier concentration ( $n_c$ ) increased from  $2.7 \times 10^{16}$  to  $8.2 \times 10^{19} \text{cm}^{-3}$ , whereas the electron mobility ( $\mu$ ) decreased from 115 to  $32 \text{cm}^2/(\text{V} \cdot \text{s})$ , respectively. The  $E_g$  of the films deposited at 200 and 300°C were determined to be 1.23 and 1.22eV, respectively.

## References

- [1] Bagnall D M, Chen Y F, Zhu Z, et al. Optically pumped lasing of ZnO at room temperature. *Appl Phys Lett*, 1997, 70: 2230
- [2] Ohtomo A, Kawasaki M, Koida T, et al. Mg<sub>x</sub>Zn<sub>1-x</sub>O as a II-VI widegap semiconductor alloy. *Appl Phys Lett*, 1998, 72: 2466
- [3] Rao V J, Salvi M V, Samuel V, et al. Structural and optical properties of Zn<sub>3</sub>P<sub>2</sub> thin films. *J Mater Sci*, 1985, 20: 3277
- [4] Li J W, Su Y K, Meiso Y. ZnS thin films prepared by low-pressure metalorganic chemical vapor deposition. *Jpn J Appl Phys*, 1994, 33: 4723
- [5] Shao L X, Chang K H, Hwang H L. Zinc sulfide thin films deposited by RF reactive sputtering for photovoltaic applications. *Appl Surf Sci*, 2003, 305: 212
- [6] Hsu T, Lin Y J, Su Y K, et al. Growth of ZnSe thin films on ITO/glass substrates by low pressure metalorganic chemical vapor deposition. *J Cryst Growth*, 1992, 125: 420
- [7] Sun X W, Xiao R F, Kwok H S. Epitaxial growth of GaN thin film on sapphire with a thin ZnO buffer layer by liquid target pulsed laser deposition. *J Appl Phys*, 1998, 84: 5776
- [8] Nakamura S, Mukai T, Senoh M. Candela-class high-brightness InGaN/AlGaIn double-heterostructure blue-light-emitting diodes. *Appl Phys Lett*, 1994, 64: 1687
- [9] Kim M H, Bang Y C, Park N M. Growth of high-quality GaN on Si (111) substrate by ultrahigh vacuum chemical vapor deposition. *Appl Phys Lett*, 2001, 78: 2858
- [10] Kuriyama K, Takahashi Y, Sunohara F. Optical band gap of Zn<sub>3</sub>N<sub>2</sub> films. *Phys Rev B*, 1993, 48: 2781
- [11] Futsuhara M, Yoshioka K, Takai O. Structural, electrical and optical properties of zinc nitride thin films prepared by reactive RF magnetron sputtering. *Thin Solid Films*, 1998, 322: 274
- [12] Toyoura K, Tsujimura H, Goto T. Optical properties of zinc nitride formed by molten salt electrochemical process. *Thin Solid Films*, 2005, 492: 88
- [13] Partin D E, Williams D J, O'Keefe M. The crystal structures of Mg<sub>3</sub>N<sub>2</sub> and Zn<sub>3</sub>N<sub>2</sub>. *J Solid State Chem*, 1997, 132: 56
- [14] Li B S, Liu Y C, Zhi Z Z, et al. Optical properties and electrical characterization of p-type ZnO thin films prepared by thermally oxidizing Zn<sub>3</sub>N<sub>2</sub> thin films. *J Mater Res*, 2003, 18: 8
- [15] Wang C, Ji Z G, Liu K, et al. p-type ZnO thin films prepared by oxidation of Zn<sub>3</sub>N<sub>2</sub> thin films deposited by DC magnetron sputtering. *J Cryst Growth*, 2003, 259: 279
- [16] Yu J, Xing H, Zhao Q, et al. The origin of additional modes in Raman spectra of N<sup>+</sup>-implanted ZnO. *Solid State Commun*, 2006, 138: 502
- [17] Ma J G, Liu Y C, Mu R, et al. Method of control of nitrogen content in ZnO films: structure and photoluminescence properties. *J Vac Sci Technol B*, 2004, 4: 94

## 衬底温度和氮气分压对氮化锌薄膜的性能影响\*

张 军<sup>1,2</sup> 谢二庆<sup>1</sup> 付玉军<sup>1</sup> 李 晖<sup>1</sup> 邵乐喜<sup>2,†</sup>

(1 兰州大学物理科学与技术学院, 兰州 730000)

(2 湛江师范学院物理科学与技术学院, 湛江 524048)

**摘要:** 采用射频磁控溅射法在不同衬底温度和不同氮气分压下在石英玻璃衬底上制备氮化锌薄膜. 利用 XRD 和喇曼散射仪分析了样品的晶体结构和组成. 结果表明当氮气分压为 1/2 时可以生成多晶单一相的氮化锌薄膜. 利用霍尔效应和光学透过谱测量了样品的电学和光学性质. 结果表明衬底温度对样品的电学和光学性质有很大的影响. 衬底温度从 100°C 上升到 300°C 时, 样品的电阻率从 0.49 降低到  $0.023 \Omega \cdot \text{cm}$ . 电子浓度从  $2.7 \times 10^{16}$  升高到  $8.2 \times 10^{19} \text{cm}^{-3}$ . 在衬底温度为 200°C, 氮气分压为 1/2 时, 样品的光学带隙为 1.23eV.

**关键词:** 氮化锌; 薄膜; 射频溅射; 光电性质

EEAC: 0520B

中图分类号: O484.1

文献标识码: A

文章编号: 0253-4177(2007)08-1173-06

\* 广东省自然科学基金(批准号: 31927)和广东省教育厅自然科学基金(批准号: 粤财教[2006]112号)资助项目

† 通信作者. Email: shaolxmail@163.com

2007-02-07 收到, 2007-03-24 定稿